

# EXPERIMENTAL RESULTS FOR THE EXTRACTION OF ESSENTIAL OIL FROM *Lippia sidoides* CHAM. USING PRESSURIZED CARBON DIOXIDE

EMBD.Sousa<sup>1</sup>, O.Chiovone-Filho<sup>1</sup>, M.T.Moreno<sup>1</sup>, D.N.Silva<sup>1</sup>,  
M.O.M.Marques<sup>2</sup> and M.A.A.Meireles<sup>3\*</sup>

<sup>1</sup>Universidade Federal do Rio Grande do Norte, UFRN, Departamento de Engenharia Química,  
DEQ/CT, Campus Universitário, Lagoa Nova, 59072-970, Natal-RN, Brazil.  
E-mail: elisa@eq.ufrn.br

<sup>2</sup>Centro de Genética, Biologia Molecular e Fitoquímica, IAC, Cx.P. 28,  
13001-970 Campinas - São Paulo, Brazil.

<sup>3</sup>Universidade Estadual de Campinas, UNICAMP, Faculdade de Engenharia de Alimentos,  
FEA, LASEFI, 13083-970, Campinas - SP, Brazil.  
E-Mail:meireles@fea.unicamp.br

(Received: July 23, 2001 ; Accepted: March 15, 2002)

**Abstract** - The odoriferous species *Lippia sidoides* Cham. is abundant in the Brazilian Northeast. Its essential oil possesses antiseptic activity due to the presence of thymol. In this work, thermodynamic and kinetic data were experimentally determined for the CO<sub>2</sub> + *L. sidoides* system. Solubility was determined using the dynamic method at pressures of 66.7 and 78.5 bar and temperatures of 283.15, 288.15, 293.15, 295.15, and 298.15 K. SFE kinetic data were obtained at 288.15 K and 66.7 bar. The composition of the multicomponent solute mixture was determined by GC-MS and compared to the composition of both the volatile oil obtained by steam distillation and the oleoresin obtained using ethanol. The SFE process yield was higher than the yield of either the steam distillation or the ethanol extraction. The solubilities were correlated using the Peng-Robinson equation of state with one binary interaction parameter for the attractive term, considering the essential oil as a pseudo-component. Sovová's model quantitatively described the overall extraction curve.

**Keywords:** SFE, extraction, high pressure, essential oil, carbon dioxide, *Lippia sidoides*.

## INTRODUCTION

The world energy crisis and the interest in pure natural products contribute to the feasibility of the process of extraction of natural products using pressurized carbon dioxide (CO<sub>2</sub>) either near the critical point or at supercritical conditions. This technique has also been diffused industrially, especially in the fields of foods, perfumes and medicines (McHugh and Krukonis, 1986). Extraction using pressurized fluids (SFE) generally does not

require removal of the solvent either in the product or in the residual solid (Brunner, 1994).

The Brazilian Northeast has a very rich flora with a variety of indigenous species. *Lippia sidoides* Cham., a plant of the *verbenaceae* family, is a bush with a brittle stem and odoriferous leaves. Its major component is thymol, a potent antiseptic of the phenol group. Thymol has strong antimicrobial action against bacteria and fungi and is responsible for the characteristic smell of *L. sidoides* (Matos, 1989; Matos, 1998). The antimicrobial activity of *L. sidoides* oil was assessed by Lemos et al. (1990). In

---

\*To whom correspondence should be addressed

Brazil, the popular name of *L. sidoides* is "Alecrim Pimenta."

In this work, experimental results for SFE extraction of *L. sidoides* essential oil using near critical CO<sub>2</sub> are presented. The thermodynamic and kinetic aspects of the SFE process were studied using an SFE unit containing a fixed bed cell at temperatures of 283.15, 288.15, 293.15, 295.15, and 298.15 K and pressures of 66.7 and 78.5 bar. Solubility data for the pseudo-ternary system, CO<sub>2</sub> + essential oil (multi-component mixture) + cellulosic structure, was measured using the dynamic method (McHugh and Krukonic, 1986).

## MATERIALS AND METHODS

### Raw Material Characterization and Preparation

The *L. sidoides* was from Mossoró (State of Rio Grande do Norte, Brazil). The leaves were dried naturally in the shade. After harvesting, the raw material was cleaned, conditioned in plastic bags under vacuum, and stored in a domestic freezer (Consul, model 280, Brazil). The humidity of the leaves was determined using the xylol distillation method (Jacobs, 1958) as recommended for odoriferous plants. For each experimental run the frozen raw material was triturated in a domestic food processor (ARNO, model PRO, Brazil) for 15 seconds. Afterwards, the triturated solid was sifted using a shaker with sieves of the Tyler series (Produtest, no. 3614) for 15 minutes. The particle size distribution adopted for the extraction experiments was a mixture composed of 50% particles of -28/ +35 mesh, 25% of -35/ +48 mesh, and 25% of -20/ +28 mesh in mass percentage.

### Characterization of the Particles and of the Fixed Bed

The true density of the triturated leaves was determined by helium pycnometry at the Chemical Facilities of the Chemistry Institute - IQ/Unicamp. The apparent bed density was calculated using the mass of solid loaded into the fixed bed cell and the cell's volume. The porosity of the bed plus the particles was calculated using the true and the apparent densities.

### SFE Experimental Equipment and Procedure

The device used for the SFE experiments is shown in Figure 1. For each load about 120 g of *L. sidoides* were used to form the fixed bed. The material was weighed and placed inside of the equilibrium cell with the aid of a funnel and

compressed with the help of a stem in order to achieve a complete and uniform accommodation of the bed.

Initially stabilization of the system was achieved by regulating it to operate at the desired temperature and pressure. Once these conditions were attained, the experimental run was begun by opening the valve placed before the equilibrium cell after having opened the downstream valves. Timing was begun at the appearance of the first drop of oil in the collector flask placed just after the micrometering valve. The flow rate of CO<sub>2</sub>, both in the totalizer and in the bubbler, was recorded at a one-minute interval. Samples were collected at predetermined time intervals. The collector flasks were closed and stored in the freezer for subsequent analysis. The assays were performed at pressures of 66.7 and 78.5 bar and temperatures of 283.15, 288.15, 293.15, 295.15, and 298.15K. The solvent flow rate varied from  $0.62 \times 10^{-5}$  to  $3.16 \times 10^{-5}$  kg/s.

### Steam Distillation and Ethanol Extraction

The essential oil from *L. sidoides* was obtained by steam distillation using the following procedure: 60 g of triturated *L. sidoides* particles (average diameter of  $0.334 \times 10^{-3}$  m) were placed inside a Mariote tube and connected to a homemade boiler. After the vapor phase flowed through the condenser, the essential oil and the water mixture were separated. The yield was calculated as the ratio between the mass of oil and the mass of feed.

The oleoresin from *L. sidoides* was obtained using ethanol (MERCK, 99.8%) and Povh's procedure (2000): 30 g of triturated *L. sidoides* plus 180 mL of ethanol were placed inside an Erlenmeyer (250 mL), covered with rubber corks, weighed and kept under agitation (190 rpm) for 8 hours in a refrigerated incubator (Tecnal, model TE-421, Brazil) at 15°C. Afterwards, the mixture was vacuum filtered. The micelle (solvent + oleoresin) was placed in a dark flask, covered, weighed, and kept under refrigeration for 24 hours. The oleoresin was quantified gravimetrically (Spricigo, 1998, cited by Povh, 2000): 20 mL of the filtered micelle was weighed using an analytical scale (AND-HR-120, Japan) in Petri plates and allowed to rest for 48 hours in a room with the air conditioning set at 18°C. The amount of solvent evaporated was then determined. The Petri plates were taken to an oven with air circulation (Marconi, model MA035, Brazil) and temperature set at 165°C for 6 hours. Afterwards, the plates were allowed to cool in a desiccator (30 minutes) and weighed. The Petri plates were returned to the oven for additional periods of 30 minutes up to constant mass.

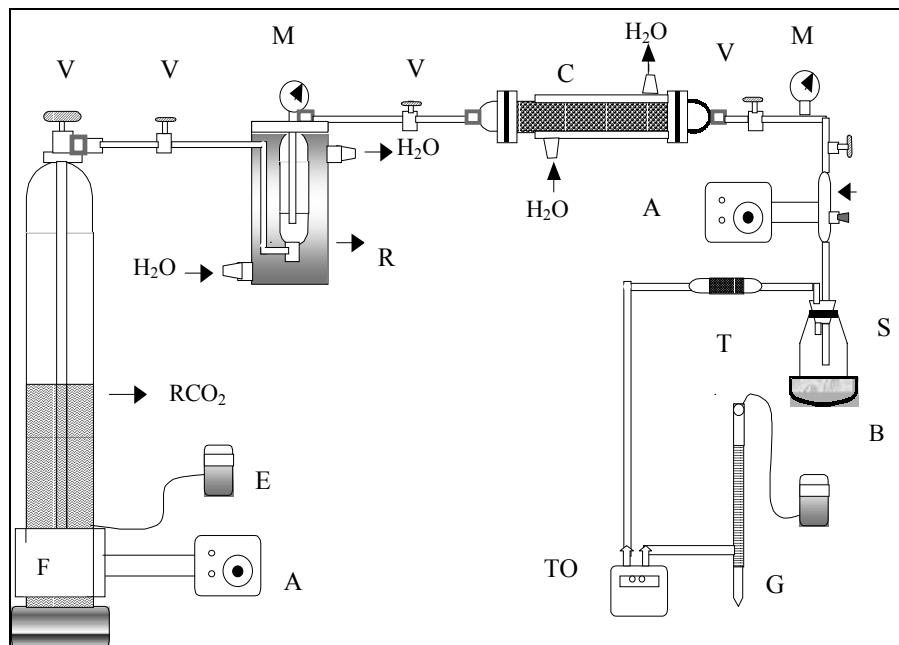


**Figure 1:** SFE unit: RCO<sub>2</sub>: CO<sub>2</sub> reservoir containing a siphon and HAVING A capacity of 25 kg;

- C = jacketed equilibrium cell or extractor made of stainless steel with length of 0.60 m, diameter of 0.0216m and wall thickness of 0.028 m;  
M = manometer Bourdon-type (RECORD, 004-99, 0 – 100 bar, Brazil);  
H<sub>2</sub>O = water bath (TECNAL, model TE 184);  
R = jacketed cylinder to maintain the solvent as a subcooled liquid with capacity of 0.5x10<sup>3</sup>;  
T = capillary glass tube filled with porapak-Q (Supelco, 80/100 mesh, 75CC, lot 113, USA);  
S = glass flask, capacity of 5 mL;  
B = glass recipient with ice cubes and water;  
A = voltage regulator (VARIAC, STP - Sociedade Técnica Paulista, model -ATV-215 M, Brazil);  
E = digital thermometer (LUTRON, model TM-905);  
F = heating tape (FISATON, model 5, Brazil);  
V = needle-type valves (HOKE, model 3712G2Y, USA);  
VM = micrometric valve (HOKE, model 1335G2Y, USA);  
G = glass bubbler; TO = flow totalizer (LAO, model G1, Brazil).

## Characterization of the Extracts from *L. Sidoides*

### (a) Chemical Composition of the Extracts

The chemical composition of the *L. sidoides* extracts was determined using a gas chromatographer coupled to a mass spectrometer system (GC-MS, Shimadzu, model QP 5000, Japan) equipped with a capillary column DB-5 (30m × 0.25 mm × 0.25µm). The carrier gas was helium (99.99% purity, White Martins Gases Industriais, 1.0 mL/min.), injector: 240 °C, detector: 230 °C. The temperature programming was from 60°C to 240°C at 3°C/min, from 240 °C to 280 °C at 10 °C/min, and remained at 280 °C for 5min. The split ratio was

1/20. The sample injected was 1.0 µL of extract diluted in ethyl acetate (0.005g of extract diluted in 1.0 mL ethyl acetate, P. A., chromatographic grade, EM Science, lot 3903991, USA). Identification of the substances was based on *i*) comparison of substance mass spectrums with GC/MS system data bank (Nist 62 Library), *ii*) comparison of mass spectrums with data from the literature (McLafferty and Stauffer, 1989), and *iii*) the retention index (Adams, 1995).

### (b) Density of the Extracts

The density of the *L. sidoides* extracts was measured using a digital densimeter (Anton Paar,

model DMA 602, Austria) at atmospheric pressure and temperatures of 283.15, 288.15, 293.15, 298.15, 303.15, and 308.15 K.

### Calculation Procedures

Using the experimental data, the overall extraction curves were fitted to a spline using two straight lines. The first line was identified with the constant extraction rate period (CER). The rate of mass transfer for the CER period ( $M_{CER}$ ) as well as the time corresponding to the interception of the two lines ( $t_{CER}$ ) was computed from the spline. The spline was fitted using multiple-regression analysis (STATISTICA 5.0). MS Excel 97 was used to determine the interception of the two lines. The mass ratio of solute in the supercritical phase at the equilibrium cell outlet ( $Y_{CER}$ ) was obtained by dividing  $M_{CER}$  by the mean solvent flow rate for the CER period.

## RESULTS AND DISCUSSION

### Solubility

The humidity of the *L. sidoides* was 9.9% (wet basis). The solid density was 1444 kg/m<sup>3</sup>, the apparent density was 546 kg/m<sup>3</sup>, and the mean particle diameter was 0.375×10<sup>-3</sup> m, resulting in a total porosity (bed + particles) of 0.62.

Typical overall extraction curves were obtained under all experimental conditions. These curves are characterized by three distinguishable regions or periods: (i) the constant extraction rate period (CER), where the solid particles can be viewed as being superficially covered by the solute; (ii) the falling or decreasing rate period (FER), where the solids have flaws in the superficial solute layer; and (iii) the diffusion controlled rate period (DCR) of an almost null rate of mass transfer, where the solute at the solid surface is exhausted, and the rate is slow due to the low diffusivity of the solute in solids. In the CER period the solute is extracted essentially by convection. In the second period the solute is extracted by both convection and diffusion. This is a transition period, caused by the exhaustion of the continuous layer of solute on the surface of the particles. Thus, mass transfer is due to both convection and diffusion. In the third period the diffusion of the solute and of the mixture of solute + solvent in the solid prevails. Figure 2 shows the comparison of the overall extraction curve obtained

at 298.15 K, 66.7 bar and 1.50×10<sup>-5</sup> kg/s with the spline fitted using two straight lines. The very last portion of the overall extraction curve, the last three experimental points (measuring time longer than 240 minutes), shows the asymptotic behavior expected for the DCR period. Nonetheless, the transition period starts after about 90 minutes, as shown in Figure 2. In the spline fitting, the key information is the slope of the first line, which was well defined by the calculation procedure employed, and, in addition, the spline quantitatively described the experimental data. Therefore, the effects of temperature, pressure and solvent flow rate on the overall extraction curves can be assessed using the spline parameters.

The solubility in liquid CO<sub>2</sub> of the essential oil present in *L. sidoides* was measured by the dynamic method, in which the solvent is saturated by the solute as it flows through the bed of solids at a predetermined constant flow rate. This methodology requires that a set of experiments be done prior to the solubility measurement in order to establish the solvent flow rate at which the solvent leaves the measuring cell under the saturation condition. This is required because at very low solvent flow rates the effects of axial dispersion will interfere with measurement of solubility. At high solvent flow rates, the contact time between the solvent and the solute will be shorter than the time necessary to saturate the solvent, and thus the mass ratio of solute at the fixed bed outlet will be smaller than the saturation value. The solvent flow rate at which saturation occurs is denoted by Q\*. In addition, the overall extraction curve should be denoted by the overall saturation curve. In the present work, the search for Q\* was performed at a pressure of 66.7 bar and a temperature of 288.15 K. The range of CO<sub>2</sub> flow rates used varied from 0.62×10<sup>-5</sup> to 3.16×10<sup>-5</sup> kg/s. Table 1 reports the results obtained and Figure 3 shows the effect of the flow rate on the mass ratio of solute in the supercritical phase at the measuring cell outlet. For experiments accomplished at extremely low solvent flow rates, the effects of axial dispersion were important, resulting in a smaller value of  $Y_{CER}$ . At high solvent flow rates, smaller values of  $Y_{CER}$  were obtained due to shorter residence times. Figure 3 shows that solvent flow rates in the vicinity of 1.50×10<sup>-5</sup> kg/s can be used to measure solubility, using the dynamic method for the *L. sidoides* + CO<sub>2</sub> system. Nonetheless, the effects of temperature and pressure on the hydrodynamics of the measuring cell must be considered: Axial dispersion is proportional to the dispersion coefficient, which is strongly dependent on the hydrodynamics of the equipment. The effects of the

thermophysical properties of the solute/solvent mixture depend on the range of temperature and pressure used. In this work, the variation in the thermophysical properties of the solute and the solvent was relatively small due to the narrow interval of both temperature and pressure. Based on this, the solubility for the *L. sidoides* + CO<sub>2</sub> system was measured at solvent flow rates in the vicinity of  $1.50 \times 10^{-5}$  kg/s.

Table 2 shows the measured solubility. In the table the amount of solute collected up to the end of the CER period (Yield<sub>CER</sub>) along with the total amount of solute collected for the entire measuring time (Yield<sub>TOTAL</sub>) is also shown. A comparison of these values with the solubility measured shows that during the entire measuring time the cellulosic structure always contain an amount of solute exceeding that required to saturate the solvent. This is a condition, which is required for use of the dynamic method in contrast to the situation found in other solid fluid processes, such as ethanol extraction, also performed in this work. Due to the strong interaction between the cellulosic structure and the solvent in low-pressure solvent extraction processes, a proportion of approximately 1:10 of solid to solvent is usually necessary. Thus, the solute + solvent mixture will always form a diluted solution, and the extraction rate will be controlled by the mass transfer restrictions. Conversely, SFE rates are controlled by both thermodynamic and mass transfer restrictions.

The effect of temperature on solubility is complex, due to the combination of two variables,

density and vapor pressure. The vapor pressure of the solute increases with temperature, causing an elevation in solubility. However, the density of the solvent decreases, thus causing a decrease in solubility. The dominant effect will depend on the magnitude of each effect on the others for each system. Higher solubility values were obtained at 66.7 bar in the range of 288.15 to 293.15 K. Therefore, the increase in the solubility for this range of temperatures should mainly be the consequence of the increase in the vapor pressure of the solute, which must have overcome the effect of lowering the solvent density. For essential oils the vapor pressure is low; however, small changes in temperature can cause significant changes in solubility. For example, a five-degrees increase in the temperature (from 288.15 K to 293.15 K) at 66.7 bar caused an increase in solubility of 14%. However, the same increase in temperature, but from 293.15 K to 298.15 K, resulted in a reduction in solubility of 42%. Therefore, in the first case the dominant effect was solute vapor pressure, while in the second it was density. The effects of both temperature and pressure on solubility can be better appreciated in Figures 4 and 5. The overall saturation curves at 66.7 bar and various temperatures (Figure 4) reflect, as expected, the behavior of solubility, since the slope of each overall saturation curve is directly proportional to solubility (See Section 2.6). Figure 5 graphically represents the effect of pressure on solubility for temperatures of 288.15 K and 293.15 K. The behavior is consistent with the literature on solid-fluid equilibria (Kurnik and Reid, 1981).

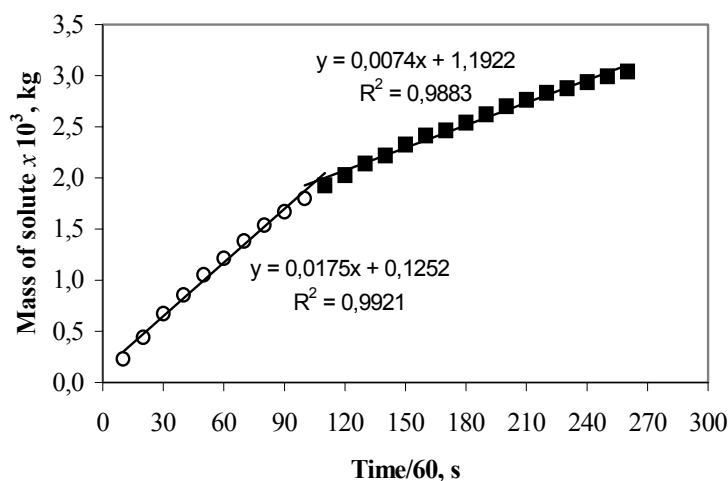


**Figure 2:** A comparison of experimental data (○, ■) with the spline fitted (—) using two straight lines at 298.15 K, 66.7 bar, and  $1.50 \times 10^{-5}$  kg/s.

**Table 1: Spline parameters for the assays performed at 66.7 bar and 288.15 K, used to choose the adequate flow rate.**

$Q \times 10^5$ kg/s	$t_{CER}/60$ s	$M_{CER} \times 10^8$ kg/s	$Y_{CER} \times 10^3$ kg/kg	Yield <sub>CER</sub> %	Yield <sub>TOTAL</sub> %
0.62	159	6.67	10.8	0.71	1.47
1.08	93	2.05	18.9	1.03	1.73
1.50	106	2.92	19.5	1.64	3.11
2.15	75	3.05	18.3	1.45	2.24
3.16	60	3.77	11.9	1.44	1.96

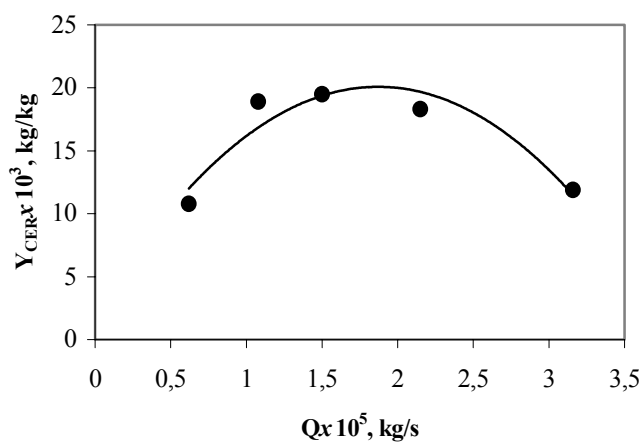


**Figure 3:** The effect of solvent flow rate on the mass ratio of solute in the fluid phase at the bed outlet at  $T=288.15$  K and  $P=66.7$  bar.

**Table 2: Solubility measured by the dynamic method for the pseudo-ternary system**

T K	P bar	$Q^* \times 10^{-5}$ kg/s	$Y^* \times 10^{-3}$ kg/kg	Yield <sub>CER</sub> %	Yield <sub>TOTAL</sub> %
283.15	66.7	1.60	13.4	1.34	2.19
288.15	66.7	1.50	19.5	1.64	3.11
288.15	78.5	1.60	17.8	1.63	3.03
293.15	66.7	1.53	22.7	1.76	3.21
293.15	78.5	1.60	20.1	1.45	2.75
295.65	66.7	1.53	19.0	1.55	3.29
298.15	66.7	1.57	13.2	1.16	2.82

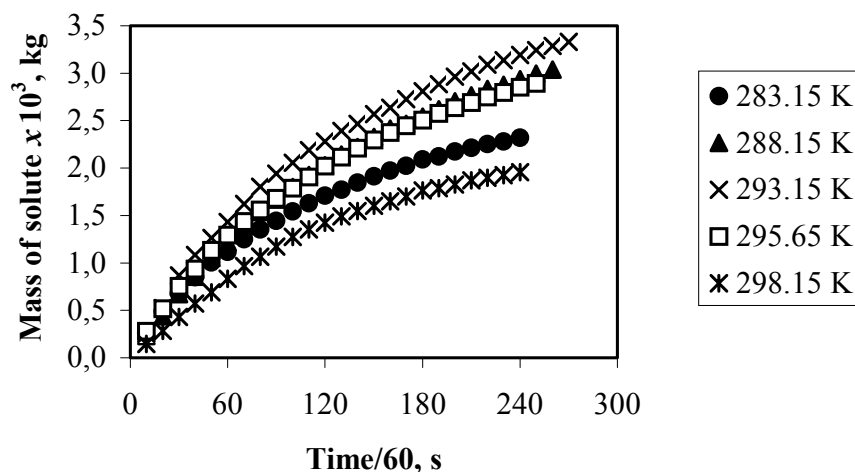


Figure 4: The influence of temperature on the overall saturation curves at 66.7 bar.

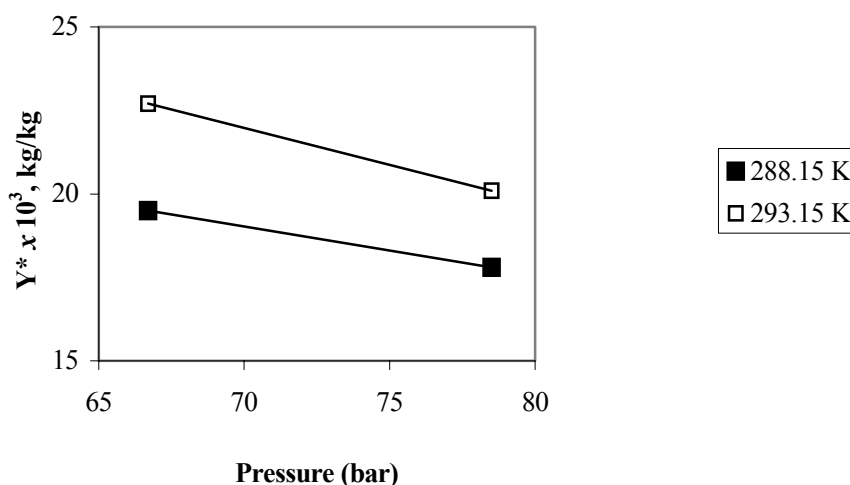


Figure 5: The dependence of solubility on pressure in the *L. sidoides* + CO<sub>2</sub> system.

### Compositions of the Essential Oil and Oleoresin

The total yields obtained in the SFE process ranged from 2.12 to 3.29% (Table 2), while the ethanol extraction resulted in a comparably lower yield (2.0%). The steam distillation process unexpectedly had a higher yield (2.4%) than the ethanol extraction process, but a lower one than that usually reported for the SFE process (Povh et al., 2001). Table 3 shows the composition of the total SFE extract obtained at 66.7 bar and 288.15 K. The compositions for the volatile oil and oleoresin are also shown in the table. In the three types of extract, monoterpene substances such as thymol, 1,8-cineole and carvacrol predominated. These last two substances are widely used by the pharmaceutical industries: 1,8-cineole, also known as eucalyptol, is used to impart flavor to various medicines, while carvacrol is employed as an anti-infection and

anthelmintic agent (Windholz, 1996).

Although thymol is the major substance present in all the extracts, the relative proportion of this compound is considerably lower in the steam distillations extract than in the other two. Conversely, the total amount of monoterpenes was approximately equal in the CO<sub>2</sub> (73.77%) and steam distillation (70.94%) extracts and was considerably higher in the ethanolic extract (85.39%). For the sesquiterpene class, the relative proportions of these compounds were similar for the CO<sub>2</sub> (20.94%) and the steam distillation (19.72%) extracts and significantly lower for the ethanol extract (5.51%). The most abundant sesquiterpene was trans-caryophyllene for the steam and CO<sub>2</sub> processes while  $\alpha$ -humulene was the most abundant one for the ethanol extraction process. The extracts also contained small amounts of eugenol, a substance that belongs to the class of phenylpropenes.

**Table 3: Components identified in the *L. sidoides* extracts.**

Component	Area %		
	CO <sub>2</sub>	Steam	Ethanol
<b>Monoterpenes</b>			
α-pinene	0.17	0.68	1.45
1-octen-3-ol	0.37	0.75	0.58
Myrcene	0.32	2.10	1.03
α-terpinene	0.12	--	0.76
Para-cymene	1.38	2.69	6.68
1,8-cineole	8.62	18.69	10.88
(E)-b-ocimene	0.50	9.86	1.64
γ-terpinene	0.58	3.25	0.28
Trans-myroxide	1.32	--	0.57
Umbellulone	0.22	--	0.05
4-terpineol	1.34	--	0.75
α-terpineol	2.27	--	1.02
Thymol, methyl ether	1.34	5.28	2.00
Thymol	48.32	22.37	50.57
Carvacrol	6.90	4.60	7.13
<b>Eugenol</b>	0.49	1.07	0.48
<b>Sesquiterpenes</b>			
α-copaene	0.26	1.04	0.10
Trans-caryophyllene	13.77	3.79	4.68
Aromadendrene	1.81	5.35	0.03
α-humulene	0.65	7.84	0.34
γ-murolene	0.26	--	0.06
α-selinene	1.72	0.83	0.23
δ-cadinene	0.59	0.87	0.07
Caryophyllene oxide	1.88	--	--
<b>Unidentified</b>	4.80	8.94	8.62

### Thermodynamic Modeling of the Solubility

As described in the previous section, the essential oil of *L. sidoides* is a multicomponent mixture formed by substances from various chemical classes. The thermophysical properties of the majority of these substances are not available. Nonetheless, for design purposes knowledge of solubility as a function of the operating conditions is required, so we should develop models to describe the behavior of solubility as a function of temperature and pressure. Since, in general, the SFE system will be designed using overall extraction curves – and consequently using the properties of the extract mixture – for the thermodynamic modeling of solubility, the oil was assumed a pseudopure component or pseudocomponent. The required thermophysical properties of the solute were evaluated using the composition shown in Table 3.

There, the composition is reported as the relative proportion or the area percent of the substances detected by the CGMS system. Despite the fact that the response factor of the various compounds may be different, as a first approximation the area percent was taken as the mass fraction of the compounds in the mixture. The required properties of each substance were either obtained from available experimental data (Daubert and Danner, 1995) or calculated using group contribution methods (Reid et al., 1987). Afterwards, Kay's rule (1936) was used, in terms of molar fraction, for the characterization of each property (M) of the pseudocomponent oil:

$$M_{\text{oil}} = \sum y_i M_i \quad (1)$$

For the normal boiling point ( $T_b$ ), critical temperature ( $T_c$ ), critical pressure ( $P_c$ ) and critical



volume ( $V_c$ ), the Joback's group contribution method (Reid et al., 1987) was used. The vapor pressures were calculated using Wagner's equation as modified by Vetere (1991). The acentric factor for each component was calculated using the following equation (Edmister and Lee, 1983):

$$\omega = \left[ \frac{3}{7} \frac{T_b/T_c}{1 - T_b/T_c} \log \left( \frac{P_{atm}}{P_c} \right) \right] - 1 \quad (2)$$

The thermophysical properties of  $\alpha$ -pinene,  $\alpha$ -terpinene, para-cimene, and  $\gamma$ -terpinene are from DIPPR (Daubert & Danner, 1995). For the other substances, the selection of the group contribution method was based on ability of the method to reproduce the experimental data for other substances found in the literature (Daubert and Danner, 1995). Table 4 shows the critical and physical properties of the compounds present in the *L. sidoides* essential oil and its pseudocharacterization using Kay's rule.

The molar volume of the essential oil was estimated using the experimental density data on the SFE extract (Figure 6) and the average molecular mass. The measured densities varied linearly with temperature for the range of conditions studied.

At constant temperature and pressure, the equilibrium equation for the essential oil (1) and  $CO_2$  (2) system is given by the equality of the fugacities in the solid substratum and fluid phases.

$$\hat{f}_i^S(T, P, x_i) = \hat{f}_i^F(T, P, y_i) \quad (i = 1, 2) \quad (3)$$

Superscripts S and F refer to the solid substratum and the fluid (liquid, gaseous or supercritical phases)

and  $x_i$  and  $y_i$ , correspond to the molar fraction in these phases, respectively. Considering that the solid substratum phase consists of an inert matrix (cellulosic structure) where the solute (pure essential oil designated by index 1) is dissolved, we have  $x_1 = 1$  and

$$y_1 = \frac{P_1^{sat} \exp \left[ \frac{V_1^{sat} (P - P_1^{sat})}{RT} \right]}{\hat{\Phi}_1^F P} \quad (4)$$

Equation (4) expresses the solubility of the oil in the fluid phase. Since it is well known that the interaction between the solute and the inert matrix or cellulosic structure cannot be neglected, the use of Equation (4) implies acceptance that this effect will be lumped together in the binary interaction parameter used to calculate the fugacity coefficient.

In order to calculate the fugacity coefficient, the Peng and Robinson (1976) equation of state was applied, using one binary adjusted parameter for the attractive term, with the following mixing rules:

$$a = \sum \sum y_i y_j a_{ij} \quad \text{for } i \neq j \quad a_{ij} = \sqrt{a_{ii} a_{jj}} (1 - k_{ij}) \quad (5)$$

$$b = \sum y_i b_i \quad (6)$$

Figure 7 shows a comparison of experimental and calculated solubility values. The calculations were done using Sandler's routines (1999). The experimental data was satisfactorily represented by the model, resulting in an average deviation of less than 10%, using estimated interaction parameter ( $k_{12}$ ) for oil- $CO_2$  equal to 0.244. This indicates that for designing purposes the procedure just described for the modeling of solubility will prove to be useful.

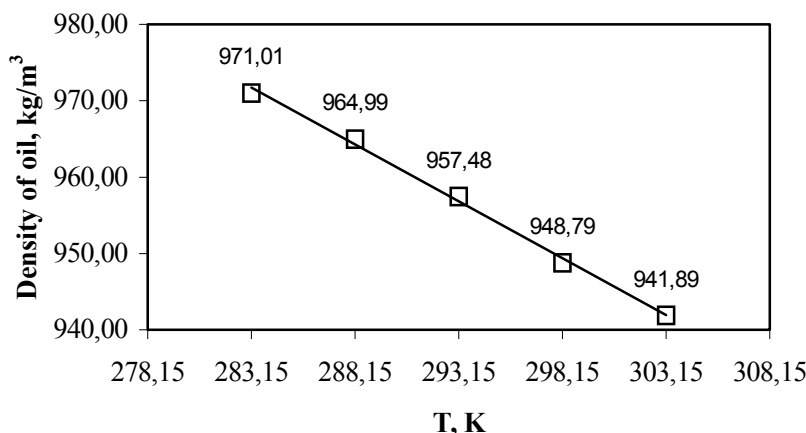


**Figure 6:** A comparison of the experimental density ( $\square$ ) of *L. sidoides* essential oil, as a function of temperature at 66.7 bar, with the fitted line ( $-$ ) ( $R^2=0.9968$ ).

**Table 4: Themophysical properties of the compounds present in the essential oil of *L. sidoides*.**

Substance	MW (g/mol)	Mole Fraction <sup>a</sup>	T <sub>b</sub> <sup>b</sup> (K)	T <sub>c</sub> <sup>b</sup> (K)	P <sub>c</sub> <sup>b</sup> (bar)	V <sub>c</sub> <sup>b</sup> (cm <sup>3</sup> /mol)	ω <sup>c</sup>
α-pinene <sup>d</sup>	136	0.0021	429.29	644.00	27.24	454.00	0.2210
1-octen-3-ol	128	0.0048	454.32	640.71	31.85	424.50	0.5642
Myrcene	136	0.0039	425.48	609.58	24.22	539.5	0.3653
α-terpinene <sup>d</sup>	136	0.0015	448.15	649.00	27.63	489.00	0.3721
Para-cymene <sup>d</sup>	134	0.0173	450.28	652.00	28.00	497.00	0.3738
1,8-cineole	154	0.0939	469.91	689.12	29.60	509.50	0.3465
(E)-b-ocimene	136	0.0062	432.96	622.27	24.46	538.50	0.3553
γ-terpinene <sup>d</sup>	136	0.0072	456.15	661.00	27.63	489.00	0.3761
Trans-myroxide	152	0.0146	458.18	657.47	26.41	532.50	0.3952
Umbellulone	150	0.0025	513.44	736.91	30.56	494.50	0.4567
4-terpineol	154	0.0146	527.33	754.31	33.22	472.50	0.5091
α-terpineol	156	0.0244	515.49	738.83	30.09	482.50	0.4568
Thymol, methyl ether	164	0.0137	509.70	716.96	25.46	555.50	0.4757
Thymol	150	0.5403	540.04	764.51	34.40	447.50	0.5784
Carvacrol	150	0.0771	540.04	764.51	34.40	447.50	0.5783
Eugenol	164	0.0050	559.58	781.18	35.10	452.50	0.6661
α-copaeno	204	0.0021	608.85	822.07	19.60	844.50	0.5744
Trans-caryophyllene	204	0.1132	576.30	802.06	20.27	716.50	0.4235
Aromadendrene	204	0.0149	556.75	772.11	19.70	709.50	0.4279
α-humulene	204	0.0053	591.18	827.88	20.57	724.50	0.3995
γ-murolene	204	0.0021	571.35	785.53	19.19	720.50	0.4603
α-selinene	204	0.0141	541.57	769.59	20.60	666.50	0.3317
δ-cadinene	204	0.0049	585.98	802.43	19.53	723.50	0.4908
Caryophyllene oxide	220	0.0143	616.00	850.16	22.38	775.50	0.5154
<b><i>L. sidoides</i> Oil<sup>e</sup></b>	<b>159.66</b>		<b>533.24</b>	<b>755.71</b>	<b>30.90</b>	<b>505.72</b>	<b>0.5145</b>

<sup>a</sup> Composition estimated using the GC-MS data (Table 3); <sup>b</sup> Critical constants estimated by the Joback group contribution method (Reid et al., 1987); <sup>c</sup> Acentric factor estimated by the Edmister and Lee expression (1983); <sup>d</sup> Experimental values retrieved from the AIChE DIPPR data bank (Daubert and Danner, 1995); <sup>e</sup> Pseudocharacterization using Kay's rule (see equation (2)).

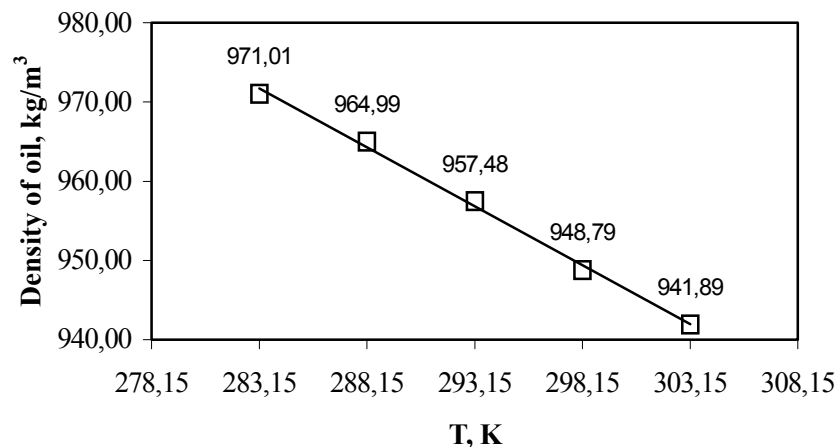


**Figure 6:** A comparison of the experimental density (□) of *L. sidoides* essential oil, as a function of temperature at 66.7 bar, with the fitted line (—) ( $R^2=0.9968$ ).

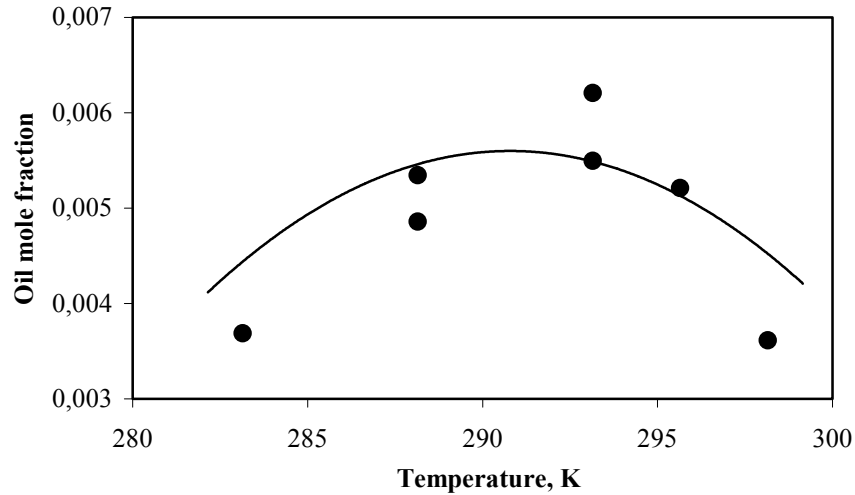


**Figure 7:** A comparison of the experimental (•) with the estimated (—) solubility using one binary parameter for the attractive term ( $k_{12}=0.244$ ).

### Modeling of the Extraction Curve

To demonstrate the usefulness of the solubility values measured in this work, the overall extraction curve obtained at 66.7 bar, 288.15 K, and  $3.16 \times 10^5$  kg/s was fitted to Sovová's model. Various models have been proposed in the literature to describe the extraction behavior of oils in supercritical and near critical fluids (Tezel and Hortaçsu., 2000, Esquivel et al., 1999 and Reis-Vasco et al., 2000). However, Lack's extended model discussed by Sovová (1994), Sovová's model, offers the advantage of providing a simple analytical solution to describe the mass balance and give a good physical description of the process. Sovová's model assumes pseudo-steady state, plug flow, and that temperature, pressure, and solvent velocity are kept constant throughout the

extraction. In addition, the bed is considered homogeneous with respect to the solute and particle size distributions. The overall extraction curves are represented by the following equations (Pasquel et al., 2000):

For the CER period,  $t < t_{\text{CER}}$

$$m_{\text{extr}} = Y^* [1 - \exp(-Z)] Q_{\text{CO}_2} \cdot t \quad (7)$$

For the FER period,  $t_{\text{CER}} \leq t < t_{\text{FER}}$

$$m_{\text{extr}} = Y^* [t - t_{\text{CER}} \cdot \exp(z_w - Z)] Q_{\text{CO}_2} \quad (8)$$

For the diffusion-controlled period,  $t \geq t_{\text{FER}}$

$$m_{\text{extr}} = N \left\langle X_0 - \frac{Y^*}{W} \ln \left[ 1 + \left[ \exp \left( \frac{W X_0}{Y^*} \right) - 1 \right] \exp \left[ \left( \frac{W \cdot Q_{\text{CO}_2}}{N} \right) (t_{\text{CER}} - t) \right] \frac{X_k}{X_0} \right] \right\rangle \quad (9)$$

where  $m_{\text{ext}}$  is the mass of extract (kg),  $N$  is the mass of inert solid (kg),  $Y^*$  is the solubility of the extract in the solvent (kg/kg),  $X_k$  is the solute mass ratio for the unruptured cells in the solid phase,  $X_p$  is the solute mass ratio for the easily accessible solute also in the solid phase, and  $X_0$  is the initial and solute mass ratio in the solid phase.  $Z = (N \cdot k_{Y_a} \cdot \rho_{\text{CO}_2}) / (Q_{\text{CO}_2} \cdot (1 - \epsilon) \cdot \rho_s)$ , where  $k_{Y_a}$  is the fluid-phase mass transfer coefficient ( $\text{s}^{-1}$ ),  $\rho_{\text{CO}_2}$  is the solvent density ( $\text{kg}/\text{m}^3$ ),  $Q_{\text{CO}_2}$  is the solvent flow rate (kg/s),  $\epsilon$  is the bed + particles porosity, and  $\rho_s$  is the inert solid density ( $\text{kg}/\text{m}^3$ ).  $W = (N \cdot k_{X_a}) / (Q_{\text{CO}_2} \cdot (1 - \epsilon))$ , where  $k_{X_a}$  is the solid-phase mass transfer coefficient ( $\text{s}^{-1}$ ). Figure 8 compares the experimental and overall extraction curves where the following parameters were used:  $Z = 0.9405$ ,  $t_{\text{CER}}/60 = 36$  s;  $t_{\text{FER}}/60 = 75$  s;  $X_p/X_0 = 0.55$ ;  $k_{Y_A} = 1.62 \times 10^{-4} \text{ s}^{-1}$ ;  $k_{X_A} = 7.58 \times 10^{-5} \text{ s}^{-1}$ .

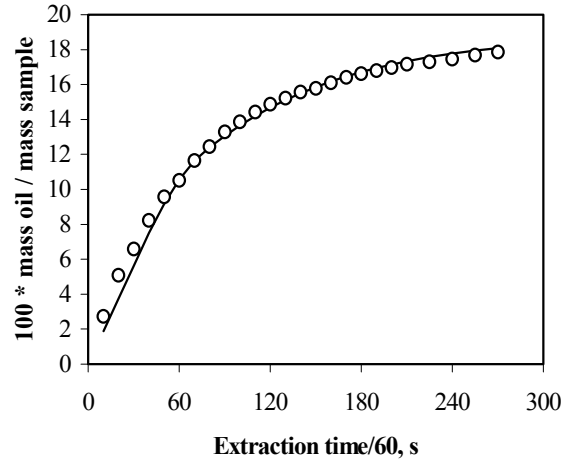


**Figure 8:** A comparison of the experimental (○) with the calculated (—) overall extraction curve at 288.15 K, 66.7 bar, and  $3.16 \times 10^{-5}$  kg/s.

## CONCLUSIONS

The use of liquid carbon dioxide at near critical conditions proved to be adequate to extract the essential oil from *L. sidoides* leaves. For the experimental setup used, the solvent flow rate which proved adequate for the solubility measurements was in the vicinity of  $1.50 \times 10^{-5}$  kg/s. The SFE process produced higher yields (3.3%) than both steam distillation (2.4%) and ethanol extraction (2.0%), but the chemical profiles of the extracts were all similar. The thermodynamic method used to estimate solubility satisfactorily described the system. Similarly, the extended Lack model, as presented by Sovová (1994), quantitatively described the overall extraction curve.

## ACKNOWLEDGMENTS

We would like to thank CNPq, FAPAM, and FAPESP (1999/01962-1) for the financial support.

## NOMENCLATURE

C	subscript for critical property
CER	constant extraction rate
D	density ( $\text{kg}/\text{m}^3$ )
F	fugacity
$J(X,Y)$	interfacial mass transfer rate
$K_{XA}$	mass transfer coefficient in the solid phase ( $\text{s}^{-1}$ )

$K_{YA}$	mass transfer coefficient in the fluid phase ( $\text{s}^{-1}$ )
$m_{\text{ext}}$	mass of extract (kg)
N	mass of inert solid (kg)
P	pressure (bar)
$Q_{\text{CO}_2}$	solvent flow rate (kg/s)
$Q^*$	solvent flow rate under saturation condition (kg/s)
$R^2$	correlation coefficient
Sat	superscript to indicate saturation property
T	temperature (K)
$t_{\text{CER}}$	time of the CER period (min)
$t_{\text{FER}}$	time of the period of decreasing rate of extraction (min)
V	molar volume ( $\text{m}^3/\text{mol}$ )
$X_K$	ratio between the mass of solute inside the cell and mass of inert solid
$X_O$	ratio between the initial mass of solute and mass of inert solid
$Y^*$	solubility (kg oil/ kg $\text{CO}_2$ )
$y_1$	mole fraction of the oil in the fluid phase
$Y_{\text{CER}}$	oil concentration at the $t_{\text{cer}}$ (kg oil/ kg $\text{CO}_2$ )
$\hat{\Phi}_1^F$	fugacity coefficient for the oil in the fluid mixture
$\epsilon$	porosity
$\omega$	acentric factor
$\Delta$	variation
$\rho_f$	density of the fluid phase ( $\text{kg}/\text{m}^3$ )
$\rho_s$	density of the solid phase ( $\text{kg}/\text{m}^3$ )

## REFERENCES

- Adams, R.P., Identification of Essential Oil Components by Gas Chromatography/Mass Spectroscopy (1<sup>st</sup> ed., p.468). Allured Publishing Corporation, Illinois (1995).
- Brunner, G., Gas Extraction: An Introduction to Fundamentals of Supercritical Fluids and the Application to Separation Processes (1<sup>st</sup> ed.). Springer, New York (1994).
- Daubert, T.E. and Danner, R.P., DIPPR Data Compilation Version 13.0. New York (1995).
- Edmister, W.C. and Lee, B.I., Applied Hydrocarbon Thermodynamics, vol. 1. Gulf Publishing Company Book Division, Houston (1983).
- Esquivel, M.M., Bernardo-Gil, M.G. and King, M.B., Mathematical Models for Supercritical Extraction of Olive Husk Oil. Journal of Supercritical Fluids 16, 43-58 (1999).
- Jacobs, M., The Chemical Analysis of Foods and Food Products, 3<sup>rd</sup> ed., pp. 22-23. Van Nostrand Reinhold Co., New York (1958).
- Kay, W.B., Density of Hydrocarbon Gases and Vapors. Ind. Eng. Chem., 28, 9, 1014-1019 (1936).
- Kurnik, R.T. and Reid, R.C., Solubility Extrema in Solid-Fluid Equilibria. AIChE Journal, 27, 861-863 (1981).
- Lemos, T.L.G., Matos, F.J.A., Alencar, J.W., Craveiro, A.A., Clark, A.M. and McChesney, J.D., Antimicrobial Activity of Essential Oils of Brazilian Plants. Phytotherapy Research, 4(2), 82-83 (1990).
- Matos, J.A., Farmácia Viva. Edições UFC (Universidade Federal do Ceará), Fortaleza, Brazil (1998).
- Matos, J.A., Plantas Mediciniais, vol. II. Edições UFC (Universidade Federal do Ceará), Fortaleza, Brazil (1989).
- McHugh, M.A. and Krukonis, V.J., Supercritical Fluid Extraction. Butterworths, New York (1986).
- McLaferty, F.W. and Stauffer, D.B., The Wiley/NBS Registry of Mass Spectral Data, Vol. 1. John Wiley and Sons, New York (1989).
- Pasquel, A., Meireles, M.A.A., Marques, M.O.M. and Petenate, A.J., Extraction of Stevia Glycosides with CO<sub>2</sub> + Water, CO<sub>2</sub> + Ethanol, and CO<sub>2</sub> + Water + Ethanol. Brazilian Journal of Chemical Engineering, 17(3), 271-282 (2000).
- Peng, D.Y. and Robinson, D.B., A New Two-Constant Equation of State. Ind. Eng. Chem. Fundam., 15, 59-64 (1976).
- Povh, N.P., Obtenção do óleo essencial de camomila *Matricaria recutita* [L.] Rauschert por diferentes métodos: Destilação por arraste a vapor, Extração com solventes orgânicos e extração com CO<sub>2</sub> supercrítico, Doctoral diss., FEA – Universidade Estadual de Campinas (UNICAMP), Campinas, SP, Brazil (2000).
- Povh, N.P., Marques, M.O.M., Meireles, M.A.A., Supercritical CO<sub>2</sub> Extraction of Essential Oil and Oleoresin from Chamomile (*Chamomilla recutita* [L.] Rauschert), Journal of Supercritical Fluids, 21(3), 245-256 (2001).
- Reid, R.C., Prausnitz, J.M. and Poling, B.E., The Properties of Gases and Liquids. McGraw-Hill, New York (1987).
- Reis-Vasco, E.M.C., Coelho, J.A.P., Palavra, A.M.F., Marrone, C. and Reverchon, E., Mathematical Modeling and Simulation of Pennyroyal Essential Oil Supercritical Extraction. Chemical Engineering Science 15, 2917-2922 (2000).
- Sandler, S.I., Chemical and Engineering Thermodynamics, 3<sup>rd</sup> ed., John Wiley & Sons, New York (1999).
- Sant'ana, H.B., Desenvolvimento de uma metodologia para determinação da solubilidade de oleoresinas essenciais em CO<sub>2</sub> pressurizado. Master's thesis, Faculdade de Engenharia de Alimentos, Universidade Estadual de Campinas (UNICAMP), Campinas, SP, Brazil (1996).
- Sovová, H., Rate of the Vegetable Oil Extraction with Supercritical CO<sub>2</sub> - Modeling of Extraction Curves. Chemical Engineering Science, 49(3), 409-414 (1994).
- Tezel, A. and Hortaçsu, A., Multi-component Models for Seed and Essential Oil Extractions. Journal of supercritical fluids, 19, 3-17 (2000).
- Vetere, A., Predicting the Vapor Pressures of Pure Compounds by Using the Wagner Equation. Fluid Phase Equilibria, 62, 1-10 (1991).
- Windholz, M., The Merck Index, Twelfth Ed. (p. 308: carvacrol; p. 661: eucalyptol). MERCK & CO., INC, New Jersey (1996).